Heliyon 10 (2024) e37304

Contents lists available at ScienceDirect

Heliyon

journal homepage: www.cell.com/heliyon

Research article

Synthesis and *in vitro* evaluation of cross-linked tragacanthin nanofibers as implants for delivery of cisplatin to hepatocellular carcinoma

Anam Shabbir [a], Mohammad Saeed Iqbal [a,*], Muhammad Zeeshan Saeed [b], Farooq Rashid [c]

[a] Department of Chemistry, Forman Christian College, Lahore, 54600, Pakistan
[b] Department of Physics, Electronics Laboratory, COMSATS University, Islamabad, Pakistan
[c] Health Physics Division, PINSTECH, P.O. Nilore, Islamabad, Pakistan

ARTICLE INFO

Keywords:
Electrospinning
Nanofibers
Tragacanthin
Drug delivery
Cisplatin
Anticancer

ABSTRACT

There is growing interest in the use of electrospun polymeric nanofibers in drug delivery systems due to their remarkable surface-to-volume ratio, which enhances the processes of drug loading, specific cell binding and proliferation. The preferred polymers for drug delivery must be biocompatible and biodegradable. Gum tragacanth is one of the materials of choice for drug delivery. This work aimed at cross-linking the tragacanthin, the water-soluble fraction of gum tragacanth, with glutaraldehyde, synthesis of the cross-linked nanofibers and evaluating their properties to encapsulate and deliver a drug using caffeine as a model drug in the first place. The nanofibers were then loaded with cisplatin and evaluated against HepG2 cell line. The drug-loaded nanofibers (dia. 0.841 μm) were prepared by electrospinning using glutaraldehyde as the cross-linker and glycerol as a plasticizer and characterized by scanning electron microscopy, Fourier transform-infrared spectroscopy, electronic spectroscopy, ^{1}HNMR, powder X-ray diffraction analysis, and thermogravimetric analysis. They released the encapsulated drugs in a sustained manner at pH 7.4 over 4.5 days (~275 h with ~80 % release) following Higuchi (cisplatin) and Hixon-Crowell (caffeine) kinetics. In a cytotoxicity assay against HepG2 cell line the cisplatin-loaded nanofibers exhibited enhanced activity compared to that with the standard cisplatin and in the caspase activity assay it activated caspase 3 to a higher extent and 8 and 9 to double the extent (4-fold) of cisplatin, suggesting a higher apoptotic activity by the nano-formulation than the standard cisplatin. Thus, nanoformulation appeared to be a potential candidate for treating hepatocellular carcinoma as an implant.

1. Introduction

Nanofibers have emerged as a promising class of biomaterials with unique characteristics such as a large surface area, high porosity, small pore size, and remarkable mechanical properties. Polymeric nanofibers produced through the electrospinning technique have gained significant attention as carriers for controlled and sustained drug delivery [1]. These nanofibers exhibit excellent

* Corresponding author. Department of Chemistry, Forman Christian College (A Chartered University), Ferozepur Road, Lahore, 54600, Pakistan.
E-mail addresses: saeediq50@hotmail.com, saeediqbal@fccollege.edu.pk (M.S. Iqbal).

https://doi.org/10.1016/j.heliyon.2024.e37304
Received 24 June 2024; Received in revised form 29 August 2024; Accepted 30 August 2024
Available online 31 August 2024

encapsulation efficiency, and remarkable mechanical strength, making them highly suitable for various drug delivery applications [2, 3]. They can encapsulate a wide range of poorly soluble drugs, thereby enhancing their bioavailability and achieving controlled release. Electrospinning is a simple, user-friendly, and low-cost method for creating nanofibers for drug delivery systems [4].

Among the nano frameworks El-Bindary et al. reported one-pot synthesis of biocompatible zeolitic imidazolate crystal [5] and zirconium based [6] metal-organic frameworks affording high loading and efficient delivery of doxorubicin. This group also reported non-metal chitosan based naogel for pH-responsive delivery of doxorubicin exhibiting enhanced efficacy and reduced toxicity *in vivo* [7]. These studies demonstrate the effectiveness of nanomaterials in targeting cancerous cells. Recently, Entezar-Almahdi et al. [8] reported receptor specific nano-hydrogel based on histidine-modified poly(aminoethyl methacrylamide) as targeted cisplatin (CDDP) delivery system. The system could respond to pH changes in the tumor microenvironment *in vivo* and efficiently target the HT29 cells. This group also reported synthesis of thermo-responsive poly(*N*-isopropylacrylamide) hydrogel for *in vitro* delivery of CDDP to MCF-7 cell line; the hydrogel was found to be suitable for treatment of breast cancer [9]. They also prepared hyaluronan-coated EDTA--modified [10] and imidazoline-modified [11] magnetic mesoporous silica nanoparticles for delivery of CDDP, which was evaluated as a multifunctional pH-responsive system for efficient drug delivery and magnetic resonance imaging. Nanoparticles and nanofibers are both promising materials in the field of drug delivery, but they have distinct characteristics and potential applications. Nanofibers offer, relatively, higher sustained release and are suitable for localized drug delivery, such as implantable devices. They provide a scaffold that can support cell growth while releasing therapeutic agents.

Mostly, the CDDP-loaded nanofibers have been prepared from relatively less biocompatible materials. Zhang et al. [12] encapsulated CDDP in polylactic acid-poly(ethylene oxide) electrospun nanofibers and evaluated them in a murine model. Ma et al. [13] reported polylactic acid-poly(ethylene oxide) nanofibers simultaneously loaded with cisplatin and curcumin for combination therapy to prevent cervical cancer recurrence after surgery. Similarly, Kaplan et al. [14] employed CDDP-loaded polycaprolactone-poly (glycerol monostearate-co-caprolactone) nanofiber meshes for prevention of lung cancer recurrence. These systems have limitations, such as their tendency to accumulate in the liver and low absorption rate following intravenous administration.

Very few reports are available where gum tragacanth has been employed in synthesizing nanofibers [15]. In cases where it has been utilized, the composites involve both of its components, i.e., the water-soluble and water-swellable fractions. Tragacanth, an edible gum consisting of a mixture of water-soluble (tragacanthin) and water-swellable (bassorin) polysaccharides [16], is a dried sap obtained from various plants of the genus *Astragalus* from the Indian subcontinent. It is an abundantly available gum that can be used for safe drug delivery. It is a cost-effective polysaccharide with desirable biocompatibility and biodegradability. Drug-loaded nanofibers from the gum have been extensively studied for their application as wound dressings [17–19]. To the best of our knowledge, there exists no study reporting the synthesis of cross-linked tragacanthin nanofibers for delivery of CDDP.

CDDP, a platinum-based chemotherapeutic molecule, is a powerful drug used against various types of cancer including ovarian, testicular, bladder, and lung cancers. It acts by damaging the DNA structure of rapidly dividing cancer cells, leading to their death. It forms DNA adducts through covalent bonding, which inhibit DNA replication and transcription, triggering a cascade of events that ultimately lead to cell apoptosis [20]. Its versatility and broad-spectrum activity have made it a cornerstone in cancer treatment regimens. However, CDDP's clinical use is not without challenges, as it can cause significant side effects such as nephrotoxicity and ototoxicity. Conventionally systemic chemotherapy is the most widely used treatment method. However, intravenously administered anticancer drugs face transport barriers before reaching the tumor site. Consequently, only a small fraction of the drugs reaches the tumor, so higher systemic doses are required, which lead to undesirable side effects in normal tissues. Local chemotherapy using polymer-based drug delivery systems is seen as a highly promising approach to enhance treatment efficacy and reduce systemic side effects. Additionally, local chemotherapy is emphasized as a potential future solution for such problems. To mitigate these adverse effects, researchers continue to explore novel drug delivery methods and combination therapies. CDDP-loaded implants have been studied for intramural chemotherapy [21]. The scaffolds studied so far for local cisplatin delivery lack required mechanical strength [22]. Moreover, the reports on intratumoral delivery of chemotherapeutic drugs in hepatocellular carcinoma are very rare [23], and, to the best of our knowledge, there is no report using CDDP-loaded nanofibers as implants. We hypothesize that such limitations could be overcome by preparing the drug-loaded cross-linked nanofibers, which are mechanically stronger than hydrogels. Therefore, in the present work, we planned to cross-link the gum tragacanth with glutaraldehyde and synthesize CDDP-loaded nanofibers using glycerol as a plasticizer. The objectives of this work were to i) explore the possibility of use of CDDP-loaded nanofibers as implants, ii) explore the use of gum tragacanth in implants due to its distinct properties being biocompatible, nonimmunogenic, nonallergic, non-tumorigenic, analgesic, anti-rheumatic, antibacterial, pseudoplastic and biodegradable [24], iii) cross-link the gum to enhance its

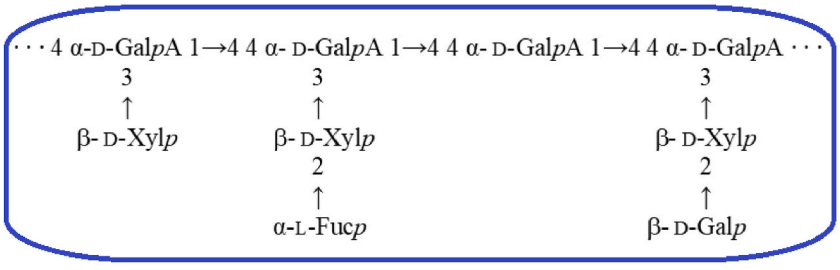

Fig. 1. Structure of gum tragacanthin [25]. Abbreviations: Gal*p* – galactopyranose, Xyl*p* – xylopyranose, Fuc*p* – fucose (6-Deoxy-galactopyranose).

mechanical strength, iv) prepare CDDP-loaded nanofibers, v) study drug release properties of the prepared nanofibers, and vi) test *in vitro* their performance against Hep G2 cell line. CDDP was selected because it is relatively more stable and can be effectively released from implants over time compared with other cytotoxic drugs like doxorubicin, which is more susceptible to degradation and can interact with the materials used in implants.

Tragacanthin (GT) consists of a linear chain of α-D-galacturonic acid residues linked at the 1 and 4 positions. The majority of these D-galacturonic acid residues are attached to sidechains containing xylose at the C-3 position. The sidechains are single β-D-xylopyranose units, as well as disaccharide units consisting of 2-*O*-α-L-fucopyranosyl-D-xylopyranose and 2-*O*-β-galactopyranosyl-D-xylopyranose with a possibility of small amounts of other units, such as xylobiose. Thus, it is a hemicellulosic material having the structure as shown in Fig. 1 [25]. The carboxylic groups of galacturonic acid residues can readily cross-link with an aldehyde through hemiacetal formation (hemiacetalization). In one example [26] the whole gum (tragacanthin + bassorin) carboxymethylated and cross-linked with glutaraldehyde. This type of cross-linking would result in the formation of a robust hydrogel. After cellulose, hemicellulose is one of the most abundant polysaccharides. However, its full potential has yet to be realized. Hemicelluloses

are partially digested in the small bowel and therefore, are generally considered as safe for drug delivery [27]. Caffeine was used, in the first place, to study the intrinsic release properties of the cross-linked nanofibers because its solubility in aqueous medium is independent of pH, then the fibers were loaded with CDDP.

Hep G2, also known as HepG2, is a cell line derived from human liver cancer. These cells serve as an *in vitro* model for studying polarized human hepatocytes and are well-suited for the study of intracellular movement of sinusoidal membrane proteins, bile canalicular and lipids within human hepatocytes [28]. So, the focus of this work was to synthesize the CDDP-loaded nanofibers and evaluate their activity against the Hep G2 cell line.

2. Materials and methods

2.1. Materials

Gum tragacanth, sodium hydroxide, glutaraldehyde (25 % aqueous solution), glycerol, methanol, caffeine, and diethyl ether were sourced from Merck, Germany, and used as received. CDDP and simulated gastric fluid without enzyme (SGF) were procured from Sigma-Aldrich, USA. The human liver cell line Hep G2 (ATCC: HB-8065™) was obtained from the American Type Culture Collection. Dulbecco's Modified Eagle Medium (DMEM), phosphate buffer saline (PBS), fetal bovine serum (10500-064 Gibco™), penicillin-streptomycin (Gibco™), trypsin (25300-054 Gibco™) and the 3-(4,5-dimethylthiazol-2-yl)-2,5-diphenyltetrazolium bromide (MTT) assay kit (Invitrogen™) were from Thermo Fisher Scientific, USA. The Mycoplasma Detection Kit MycoAlert® (Lonza Group, Ltd.), the proteasome inhibitor MG132 (Millipore-Sigma) and the caspases 3, 8, and 9 colorimetric protease assay kit (MBL, Nagoya, Japan) were used for bioassays. Distilled water was utilized throughout this work, whereas, for cell culture sterile distilled water was used.

2.2. Extraction of tragacanthin from crude gum tragacanth

The crude gum tragacanth (1.0 g) was powdered and washed with ethanol. To this water (200 mL) was added and the mixture was shaken in a sealed bottle overnight. The water-soluble fraction (tragacanthin) was separated by centrifugation at 3600×*g* for about 3 h and freeze dried for subsequent use. For freeze-drying the sample was frozen at −70 °C and then evacuated at 0.1 mbar by FD 8512 freeze dryer (ilShinBioBase, Korea) for two days. The yield was ~85.2 %.

2.3. Synthesis of cross-linked nanofibers

The freeze-dried tragacanthin (0.5 g) was mixed with 50 mL of water and 1.0 mL of NaOH solution (2.5 % w/v) was added. The resulting mixture was vigorously stirred for 10 min followed by addition of 50 mL of distilled water and stirring for 10 min. After that, additional amounts of GT (0.5 g) and NaOH (1 mL of 2.5 % w/v solution) were introduced. Following a 20-min interval, another 0.5 g of GT and 0.5 mL of glutaraldehyde (equivalent to 0.15 g) were added. The mixture was stirred for 20–30 min followed by addition of 50 mL of water, 1.5 g of GT, 2 mL of methanol and 3–4 drops of glycerol (as a plasticizer). Finally, caffeine (0.9 g) was added, and the solution was stirred for a further 20 min. The viscosity of the mixture was ~800 mPa S and conductivity ~1.0×10^{-8} S/m. The mixture for CDDP-loaded nanofibers was similarly prepared by replacing caffeine with CDDP (20 mg) and including NaCl (10 mg) to prevent transplatin formation in solution [29] as transplatin is clinically ineffective. This mixture was subjected to electrospinning.

A 10-mL polypropylene syringe (BD, Shandong, China) was filled with the electrospinning mixture, avoiding the introduction of air bubbles. The syringe was then fitted with a 24-gauge SS single needle. The needle was attached to the positive terminal of a high voltage DC power supply, and a rotating drum collector (effective length 100 mm, ø 40 mm, speed: 100–1000 r min^{-1}) wrapped in aluminum foil was grounded. The electrospinning conditions were set to: temperature 25 ± 1 °C, 35 % relative humidity, spinning distance 12 cm, voltage 10 kV DC, current < 1 mA, and pump speed 1 mL h^{-1}. The machine was assembled in the house. The nanofiber mats thus obtained were subjected to elemental analysis, scanning electron microscopy (SEM), Fourier transform-infrared spectroscopy (FT-IR), UV–Vis spectroscopy, ^{1}HNMR, powder X-ray diffraction (*p*XRD) analysis and thermogravimetric analysis (TGA) before biological testing.

2.4. Elemental analysis

Elemental analysis was performed by TruSpec Micro CHNS analyzer (LECO Corporation, USA).

2.5. FT-IR spectroscopy

The FT-IR spectra were recorded by Cary 630 FT-IR spectrometer (Agilent, USA). The sample was placed on the Diamond-ATR crystal and the spectra were recorded in the 400–4000 cm^{-1} range.

2.6. Thermogravimetric analysis

The TGA thermograms were recorded by SDT Q600 simultaneous analyzer (TA Instruments, USA) in the ambient to 800 °C range @ 20 °C min^{-1} under nitrogen flow (10 mL min^{-1}).

2.7. Powder X-ray diffraction

The *p*XRD spectra were recorded by D2 Phaser XRD spectrometer (Bruker, USA) using Cu-Kα radiation (λ = 1.54056 Å), at 40 kV and 100 mA, in the 2θ range of 5–70°.

2.8. ^{1}HNMR spectra

The ^{1}HNMR of the synthesized adduct, starting material and drug were recorded by using 60PRO 60 MHz NMR spectrometer (Nanalysis Carporation, Canada) in D_2O.

2.9. Scanning electron microscopy

The SEM images were obtained by FEI Nova NanoSEM450 scanning electron microscope (Thermo Fisher, USA).

2.10. Zeta potential measurement

Zeta potential of CDDP-loaded nanofibers was determined by Zetasizer (Zetasizer Nano ZS, Malvern Instrument Ltd., Worcestershire, UK) at 25 °C. For this, aqueous suspension of the fibers was sonicated for 30 s, transferred to disposable cuvette, and measurement was made in triplicate using 632.8-nm laser at the scattering angle of 173°. The results were reported as mean ± SD.

2.11. Degree of swelling

The degree of swelling is a relative indicator of how tightly the nanofibers are linked together. This was determined in distilled water at 37 °C by gravimetric method. The dry nanofiber mats (2 × 1.5 cm^2) were weighed and soaked in water for 2 h at 37 °C. The mats were carefully pulled out of the water and the surface water was wiped away with the help of filter paper. The wet mats were weighed again, and the degree of swelling was calculated using the formula: Degree of swelling (%) = $(M_s - M_d) \times 100/M_d$, where M_s is the weight of the swollen sample and M_d is the weight of the dry sample.

2.12. Drug-loading efficiency

The drug-loading efficiency of the cross-linked nanofibers was determined by formula: Drug loading efficiency, DLE (%) = (Amount of drug in the nanofibers/Initial amount of drug) × 100. The amount of drug in dry nanofiber mats was determined by dissolving the dry mat (24.0 mg) in 15 mL water (for caffeine) and 15 mL 0.1%HCl (for CDDP) with sonication for 5 min followed by filtration through 0.54-μm membrane filter and HPLC analysis according to USP–NF 2024. The drug standards used were 0.1–1.0 mM solutions prepared from reference materials. The amount of the drug was determined from the calibration curve exhibiting high linearity ($R^2 >$ 99.99). HPLC analysis was performed using the following.

2.12.1. For caffeine

Buffer: 0.82 g L^{-1} of anhydrous sodium acetate.
Mobile phase: acetonitrile, tetrahydrofuran, and the buffer in the ratio 25:20:955; the pH adjusted with glacial acetic acid to 4.5.
Detector: UV 275 nm.
Column: 4.6 mm × 15 cm ODS.
Flow rate: 1 mL min^{-1}
Injection size: 10 μL.

2.12.2. For cisplatin

Mobile phase: degassed mixture of ethyl acetate, methanol, dimethylformamide and water (25:16:5:5).

Detector: UV 310 nm.

Column: 4.0 mm × 30 cm monomolecular layer of aminopropylsilane chemically bonded to totally porous silica gel support (Merck KGaA, Darmstadt, Germany)

Flow rate: 2 mL min^{-1}

Injection size: 10 μL.

2.13. Drug assay in the nanofibers up to six months

In order to assess the long-term availability of the drugs in nanofibers, the drug assay was carried out periodically by HPLC for six months on the samples stored at 30 ± 1 °C in the dark for six months.

2.14. Drug release study

Drug release was studied at pH 7.4 (PBS), 5.5 (PBS) and 1.8 (SGF). A dialysis bag (MW 3500 Da) filled with the drug-loaded nanofiber (20 mg) was immersed in the dissolution medium (50 mL) and stirred (90 rpm) magnetically at 37 °C. Samples (2 mL) were withdrawn after 30, 90, 150, 210 and 270 min so on up to 240 h and assayed by USP HPLC methods as described above. Following each withdrawal, an equivalent volume of dissolution medium was added. The experiment was conducted in triplicate. The cumulative release vs time was graphed, and the data were analyzed.

2.15. Cell culture

The Hep G2 cells were cultured in DMEM supplemented with 10 % FBS and 1 % penicillin/streptomycin. The cells were maintained in a controlled environment with 5 % CO_2 at 37 °C. When cell confluence reached 85–90 %, they were detached using 0.25 % w/v trypsin and subcultured at a 1:4 ratio. Regular testing for mycoplasma contamination was performed using the MycoAlert® kit at three-month intervals. Prior to commencing the study, cell line identity was confirmed through single tandem repeats profiling. Subsequently, HepG2 cells were exposed to 10 μM of the proteasome inhibitor for a duration of 6 h prior to conducting the *in vitro* SUMOylation assay.

2.16. Cytotoxic assay

Cells nearing confluence were treated with various concentrations of sterilized (by filtration through sterile 0.2 μm Millipore Millex® hydrophilic PTFE syringe filter SLLG025SS) test samples for 24 h and relative number of viable adherent cells was determined by MTT assay. Briefly, the cells were incubated for 4 h with a 0.2 mg mL^{-1} MTT solution in the culture medium. Following a single wash with PBS, the cells were lysed using DMSO, and absorbance (at 540 nm) of the cell lysate was measured using a microplate reader (Labsystems Multiskan, Biochromatic Labsystem, Japan). The 50 % cytotoxic concentration (CC_{50}) was determined by using the dose-response curve.

2.17. Determination of caspase activity

The cells were subjected to PBS washing and then lysed using a lysis solution (MBL, Japan). Following a 10-min incubation on ice and subsequent centrifugation at 15,000×*g* for 10 min, the resulting supernatant was collected. To the lysate (50 μL), equivalent to 100 μg of protein, 50 μL of the reaction buffer (MBL, Japan) containing the specific substrates [caspase 3 (DEVD-pNA, p-nitroanilide), caspase 8 (IETD-pNA), or caspase 9 (LEHD-pNA)] was added. This mixture was incubated for 4 h at 37 °C, and the absorbance at 405 nm resulting from the liberated chromophore pNA was quantified using the microplate reader. The relative caspase activity was determined by comparing the absorbance of pNA from an apoptotic sample with that of an uninduced control and reported as percent of the control [30].

2.18. Statistical analysis

All the experiments were performed in triplicate and analyzed statistically using GraphPad Prism 8.0.1 (GraphPad Software, Inc.; Dotmatics). The results were reported as mean ± standard deviation. One-way ANOVA was used to analyze the difference between the groups.

Table 1
Elemental analysis (%) of gum tragacanth and drug-loaded nanofibers.

Material	C	H	N
GT-nanofiber	40.97	5.11	Not detected
Caffeine-nanofiber	43.25	5.35	7.41
CDDP-nanofiber	40.01	5.00	2.51

3. Results and discussion

3.1. Elemental analysis

The CHN percentages increased in Caffeine-nanofiber as the molecule of caffeine contains these elements, while in CDDP-nanofiber the CH percentages decreased and that of N increased due to absence of C and presence of NH_3 and Pt in CDDP (Table 1). Thus, the comparison of the elemental analysis values showed that the drugs are loaded on the synthesized nanofibers without degradation of the polymer.

3.2. FT-IR spectroscopy

The major absorbance bands in the spectrum of GT-nanofiber were observed at about 3435, 2930, 2860, 2150, 1745, 1380, and 1037 cm^{-1} (Fig. 2, Table 2). The broad band at ~3435 cm^{-1} was assigned to the ν(OH) in the cross-linked GT-nanofiber. The bands at ~2930 and ~2860 cm^{-1} corresponded to the $\nu_{as}(CH_2)$ and $\nu_s(CH_2)$ vibrations of methylene groups, respectively. The broad band at 2150 and 1745 cm^{-1} arose from various carbonyl species in the nanofiber. The band at ~1145 cm^{-1} corresponds to the ν_{as}(COC) of the glycosidic groups of the polysaccharide. Cross-linking of glutaraldehyde was through hemiacetalization with the -OH groups of the polysaccharide (Fig. 3). The symmetrical stretch of the carboxylate group appeared at 1380 cm^{-1}. The peaks at ~1037 cm^{-1} were due to the ν(CO) vibrations of polyols.

In the spectrum of caffeine (Fig. 2, Table 2) a broad peak was observed at 3408 cm^{-1} due to ν(NH) vibration. The peak at 1660 cm^{-1} is due to −C=N ring stretching [31]. The spectrum of CDDP exhibited absorptions due to ν_s(NH) at 3225 cm^{-1}, ν_{as}(NH) at 3315 cm^{-1}, $\delta_s(NH_3)$ at 1296 cm^{-1}, $\delta_{as}(NH_3)$ at 1640, 1585, 1540 cm^{-1}. Most of the absorption bands in the spectra of the drugs and the blank GT nanofibers were present in the drug-loaded nanofibers with no significant change (Fig. 2, Table 2) indicating that the drugs were encapsulated in the fibers without any chemical interaction. The absence of the chemical interaction suggests that synthesized

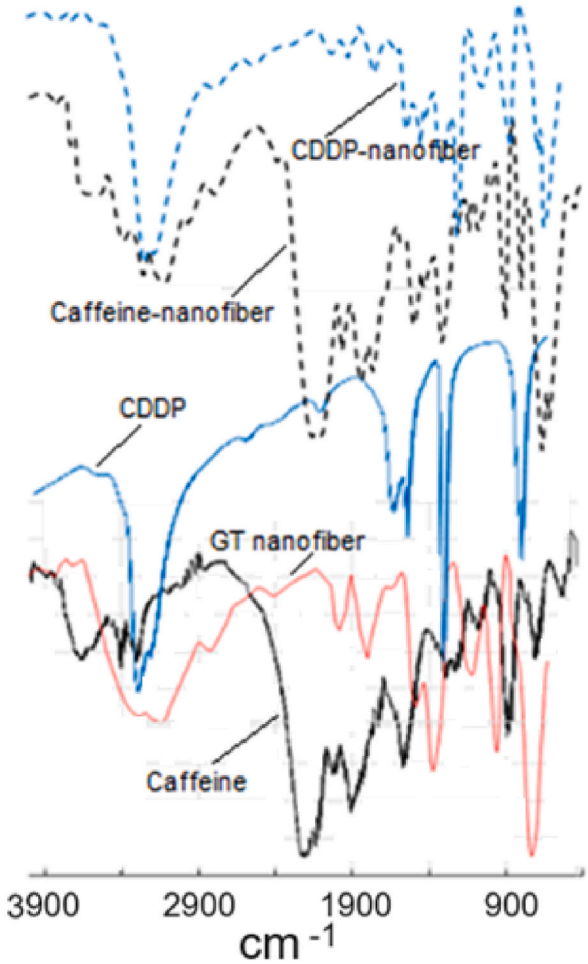

Fig. 2. FT-IR spectra of caffeine, CDDP, GT-nanofiber (blank), Caffeine-nanofiber and CDDP-nanofiber.

Table 2
FT-IR absorption bands (cm^{-1}) in the spectra of GT-nanofiber, caffeine, CDDP, Caffeine-nanofiber and CDDP-nanofiber and their assignments [31].

Material→ Band↓	GT-nanofiber	Caffeine	CDDP	Caffeine-nanofiber	CDDP-nanofiber
ν(CO) in various carbonyl species and polyols	1037, 1745, 2150	1120, 1220, 1599, 1660		1037, 1122, 1219, 1379, 1661, 1745, 2149	1038, 1121, 1218, 1380, 1748, 2150
ν_{as}(COC) glycosidic	1145			1144	1145
ν(OH)	3435			3434	3433
$\nu_s(CH_2)$	2860			2858	2858
$\nu_{as}(CH_2)$	2930			2931	2929
ν_s(N–H)			3220		3220
ν_{as}(N–H)		3408	3314		3315
$\delta_s(NH_3)$			1296		1294
$\delta_{as}(NH_3)$			1541, 1585, 1640		1540, 1583, 1641
Pyranose ring	628			625	627
ν(Ar-H)				3104, 2953	
ν(Ring -CN)	1600	1660		1637, 1660	1601
ν(-C=N)				1600	

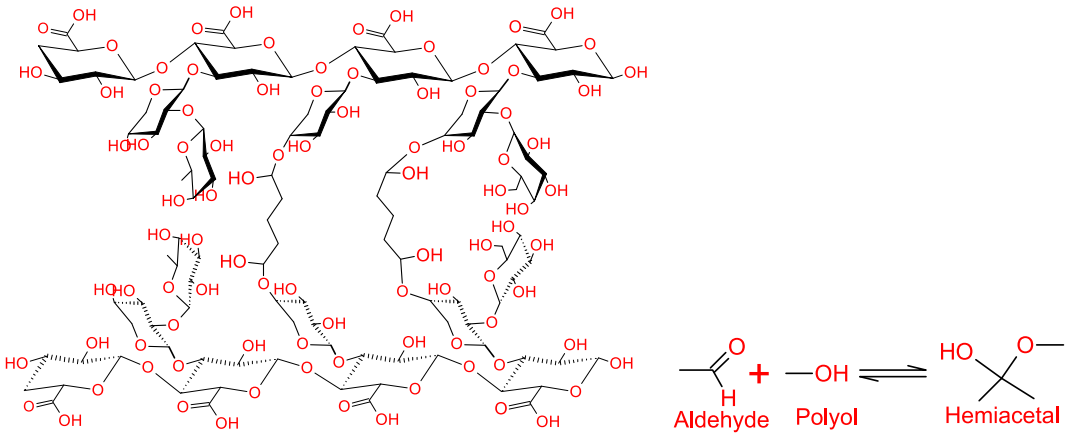

Fig. 3. Structure of GT-nanofiber cross-linked with glutaraldehyde through hemiacetal formation.

nanofibers are compatible with the loaded drugs.

3.3. Thermogravimetric analysis

Thermograms (TGA) of the drugs, blank nanofibers and drug-loaded nanofibers are shown in Fig. 4. It was observed that the drugs undergo degradation starting at ~180 °C (caffeine) and ~320 °C (CDDP), whereas in case of the blank and the drug-loaded nanofibers degradation started at ~60 °C (GT-nanofiber), ~150 °C (Caffeine-nanofiber) and ~240 °C (CDDP-nanofiber) with different patterns representing different phases due to encapsulation of the drugs. The CDDP-nanofiber exhibited higher stability (decomp. ~240 °C)

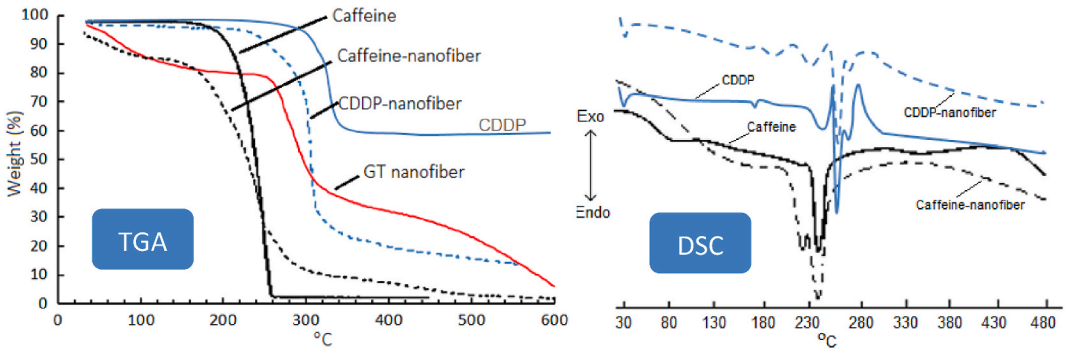

Fig. 4. Thermograms (left: TGA, right: DSC) of caffeine, CDDP, GT-nanofiber (blank), Caffeine-nanofiber and CDDP-nanofiber.

than those loaded with caffeine (decomp. ~150 °C) possibly due to stronger hydrogen bonding in the former. The CDDP-nanofiber composite afforded higher residue due to the presence of Pt. The DSC scans (Fig. 4) of caffeine-loaded and CDDP-nanofiber contained the endotherms at 235 °C and 270 °C representing the melting of caffeine and CDDP, respectively, which demonstrated the absence of any chemical interaction of the drugs with the nanofiber material.

3.4. Powder X-ray diffraction

The *p*XRD spectra of caffeine, CDDP, GT, cross-linked GT-nanofiber, Caffeine-nanofiber, and CDDP-nanofiber are shown in Fig. 5. The peaks at 20.6° and 21.9° in the spectrum of GT indicate the crystalline nature of the gum [32]. In the spectrum of cross-linked nanofibers these peaks shifted to slightly higher values in addition to broadening pattern, suggesting a reduction in crystallinity on cross-linking through hemiacetalization resulting in a relatively more amorphous three-dimensional network.

3.5. ^{1}HNMR spectra

The ^{1}HNMR spectra of caffeine, CDDP, GT-nanofiber (blank), Caffeine-nanofiber and CDDP- nanofiber are shown in Fig. 6. In the spectrum, of caffeine the chemical shifts, δ_H, at 3.4, 3.5 and 4.0 ppm correspond to CH_3-N_1, CH_3-N_3 and CH_3-N_7 respectively (refer to the structure **I** for numbering). The δ_H at 4.1 in the spectrum of CDDP is due to the NH_3 protons. These peaks are also present in the respective drug-loaded GT-nanofiber. Slight shifts in the absorptions of the blank GT-nanofiber were observed due to hydrogen bonding with the drug molecules in the spectra of the drug-loaded nanofibers (see Fig. 6).

3.6. Scanning electron microscopy

The images of the drug-loaded electrospun nanofibers are shown in Fig. 7. They appeared to be tubular in shape having porous and smooth surface with average diameters of 120 nm (Caffeine-nanofiber) and 50 nm (CDDP-nanofiber). The tubular shape ensured high drug loadings. The drugs appear to be uniformly dispersed in the tubes.

3.7. Zeta potential measurement

Zeta potential values reflect the stability of nano materials. The CDDP-loaded nanofiber exhibited a value of -25.10 ± 4.31 mV, which indicates that they are quite stable [33].

3.8. Degree of swelling

The degrees of swelling were: blank cross-linked GT-nanofiber 500 ± 5 %, caffeine-nanofibers 485 ± 4 % and CDDP-nanofiber 490 ± 4 % (n = 3). The relatively higher values are because of the tubular structure of the synthesized cross-linked GT-nanofibers that provided larger space for swelling.

3.9. Drug-loading efficiency

The drug loading efficiencies were 96.3 % (caffeine) and 97.1 % (CDDP), which showed that the cross-linked GT-nanofibers had

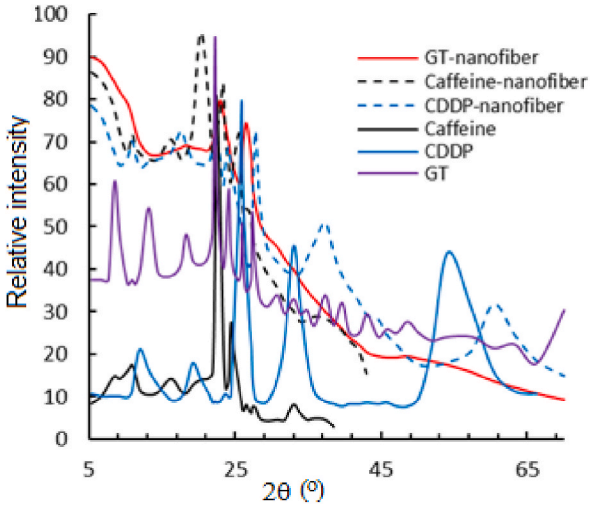

Fig. 5. *p*XRD Spectra of caffeine, CDDP, GT (bulk), cross-linked GT-nanofiber, Caffeine-nanofiber, and CDDP-nanofiber.

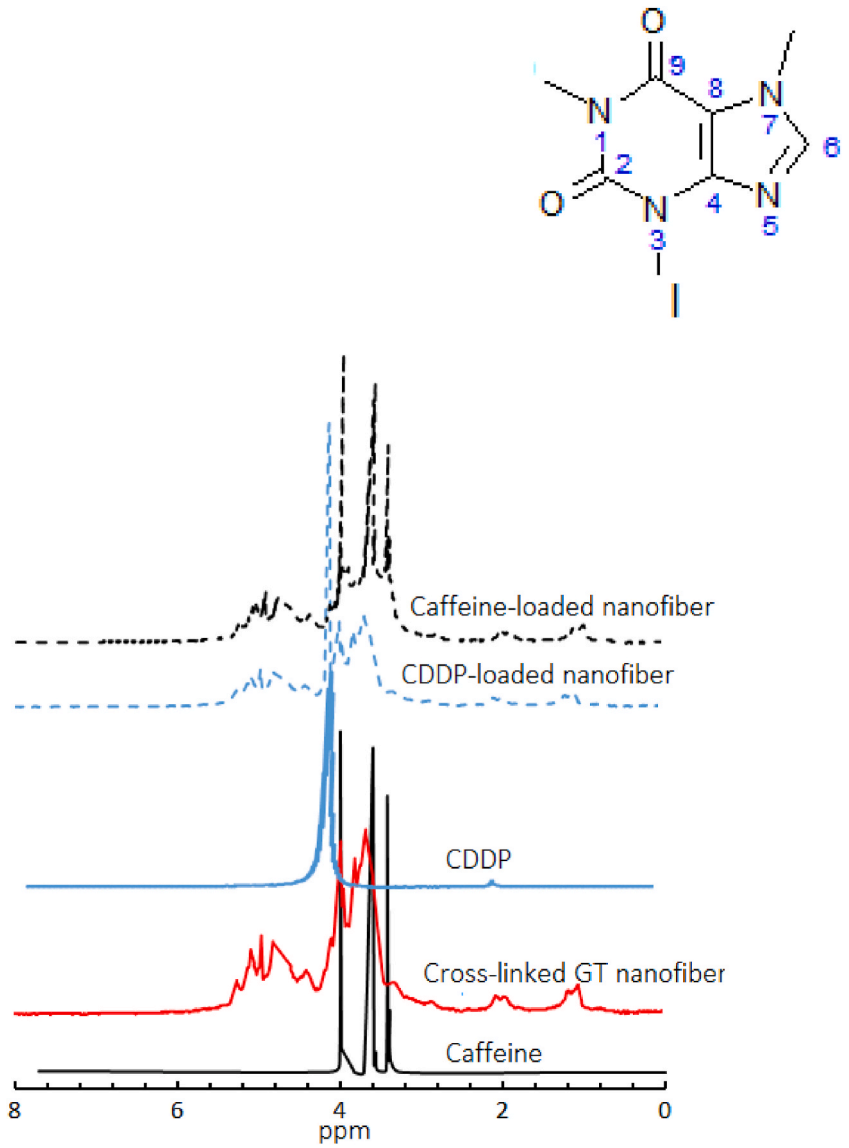

Fig. 6. ^{1}HNMR spectra (60 MHz, in D_2O) of caffeine, CDDP, GT-nanofiber (blank), Caffeine-nanofiber and CDDP-nanofiber.

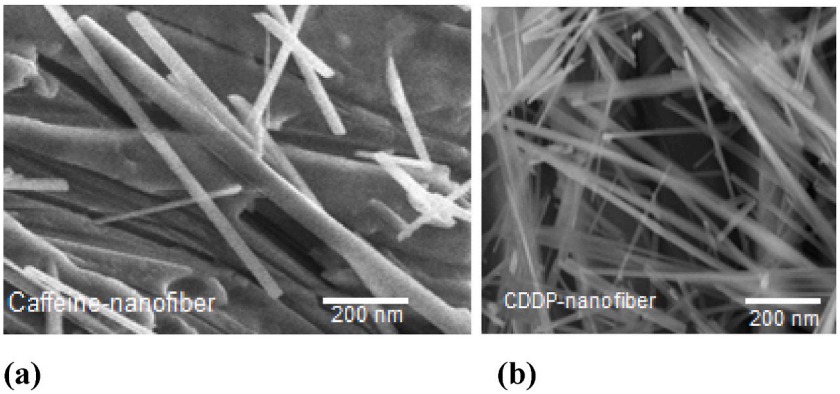

Fig. 7. SEM images of drug-loaded GT-nanofibers. (a) Caffeine loaded, (b) CDDP loaded.

high entrapment capacity due to their tubular structure. The loading efficiency of the nanofibers under investigation was close to that reported for CDDP-loaded poly-caprolactone/chitosan nanofibers (98.6 %) [34].

3.10. Drug assay in the nanofibers up to six months

The assay data is graphed in Fig. 8, which demonstrates that both the drugs remained >92 % for six months at 40C and 70 % ERH. It is worth mentioning here that there were no signs of isomerization of cisplatin during the process to transplatin as the peak due to the later was not detectable in the HPLC chromatogram of CDDP-nanofiber. Based on these results it can be predicted that the formulations will remain useable for 2–3 y if stored in a cold and dry place.

3.11. Drug release study

As caffeine exhibits a pH-independent solubility profile (Fig. 9), it was chosen as a model drug to assess the intrinsic release properties of the synthesized cross-linked GT-nanofibers at various pH values. Both drugs under investigation are released in a sustained manner for more than 240 h (Fig. 9) following the Higuchi kinetic model with $R^2 > 0.99$ [35]. So, the release appears to be controlled by diffusion and solubility. The release profiles of Caffeine-nanofiber at different pH values suggest that the drug is released at relatively higher rates with increasing pH; this is attributed to the fact that nanofibers were insoluble at pH < 7. CDDP is released, relatively, at higher rates at pH < 7 because of its higher solubility in acidic medium. The sustained release of CDDP at pH 5.5 for an extended period of time, where the release reaches ~90 % after 240 h, is of significance to its sustained cytotoxic effect on the cancer cells where the pH is around 5 [36]. At lower pH, a negligible burst release was observed against a reported value of 30 % for CDDP-loaded poly-caprolactone/chitosan nanofibers [34]. Other attempts to control this using metal-based, 3D-printed titanium alloy implants, also resulted in a burst release of CDDP [37].

3.12. Cytotoxic assay

CDDP-nanofiber showed significantly higher ($P < 0.05$) cytotoxic activity against HepG2 cells ($CC_{50} = 8 \pm 0.2$ μM, n = 3) than the CDDP standard ($CC_{50} = 13 \pm 0.4$ μM, n = 3) and the blank GT-nanofiber did not show any activity (Fig. 10). The nanofiber having a high surface area to volume ratio supports cell attachment, proliferation, drug loading, and mass transfer processes. Our CC_{50} value is close to that reported for bare CDDP (12 μM) against human hepatoma and oral squamous cell carcinoma cell lines [38], meaning by that the efficacy of the drug is not sacrificed on incorporation into the nanofibers under investigation. Other studies with different types of nanofibers [34,39,40] also support our findings.

3.13. Caspase activity

The caspases 3, 8, and 9 were activated both by CDDP-nanofiber and CDDP when incubated with HepG2 cells, while the blank GT-nanofiber did not show any activity. The activity of CDDP-nanofiber and CDDP increased with time up to 36 h and decreased afterwards (Fig. 11). Caspase 3 was activated 16-fold by CDDP compared to the control, whereas the activation of 8 and 9 was much lower (~2-fold) than this. On the other hand, the CDDP-nanofiber activated 8 and 9 to double the extent (4-fold) of CDDP. These results also show better activity than that exhibited by bare CDDP (ca. 11-fold for caspase 3) against human hepatoma and oral squamous cell carcinoma cell lines [38], Upon exposure to anticancer drugs, the cellular caspases undergo activation. The activation cascades are regulated through two pathways: an extrinsic pathway that operates outside the mitochondria, initiated by death receptors (Fas) involving caspase 8 [41], and an intrinsic pathway that takes place within the mitochondria, involving caspase 9 [42]. It has been postulated that the Fas/FasL system plays a role in modulating cell death induced by anticancer drugs [43–45]. These results suggest that the CDDP-nanofiber induces higher apoptotic activity than the CDDP standard. This induction is contingent upon the characteristics of the GT-nanofiber.

There are different pathways leading to apoptosis by CDDP. One of the critical mechanisms involves the activation of caspases. By this, CDDP binds to DNA and forms DNA adducts leading to DNA damage as reported by others [46]. This damage triggers the activation of the tumor suppressor protein p53, which leads to the transcription of pro-apoptotic genes, like Bax and PUMA, which promote the intrinsic pathway of apoptosis. The biological activity of CDDP is affected by the solvent used in a formulation. It is less soluble in water and more soluble in saline or slightly acidic solutions. Therefore, in the case of implants the drug is in the right environment, where it can undergo hydrolysis replacing chloride ligands with water molecules, which is necessary for its activation. On the hand, nucleophilic solvents can form inactive complexes, reducing their therapeutic effectiveness. The release mechanism of the drug from nanofibers may be postulated as the result of hydrolysis of CDDP at pH ~5 that the pH of cancer cells [36]. The chloride ions in the drug are replaced with water molecules; this process activates the drug action.

4. Conclusion

Electrospun glutaraldehyde cross-linked nanofibers (dia. 0.841 μm) of gum tragacanthin were prepared, and their intrinsic drug release properties were studied using caffeine as a model drug. Subsequently, the nanofibers were loaded with cisplatin. The drug loading efficiency was found to be >96 % and degree of swelling of the drug-loaded nanofibers was around 500 %. They released the encapsulated drugs in a sustained manner at pH 7.4 over 4.5 days (~275 h with ~80 % release). The release of cisplatin at pH 1.8 was

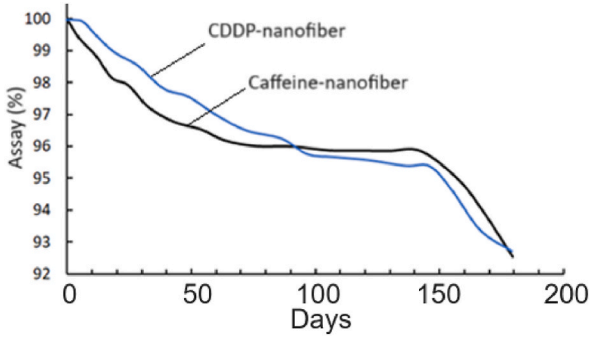

Fig. 8. Stability curves of Caffeine-nanofiber and CDDP-nanofiber.

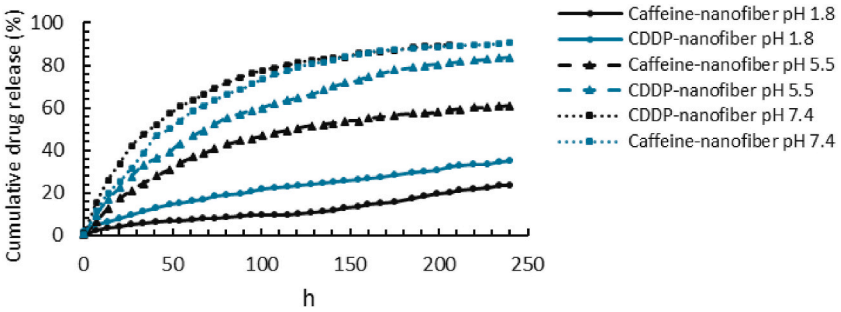

Fig. 9. Release profiles of Caffeine-nanofiber and CDDP-nanofiber at pH 1.8, 5.5 and 7.4.

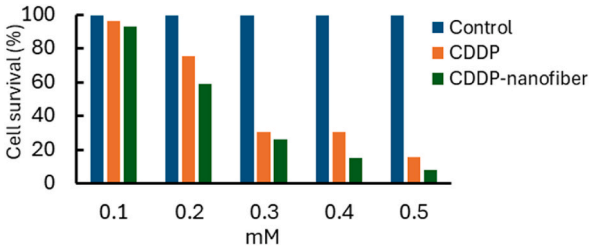

Fig. 10. Cytotoxic activity of HepG2. The cell line was incubated with the test samples for 24 h and the relative viable cell number was determined by MTT assay.

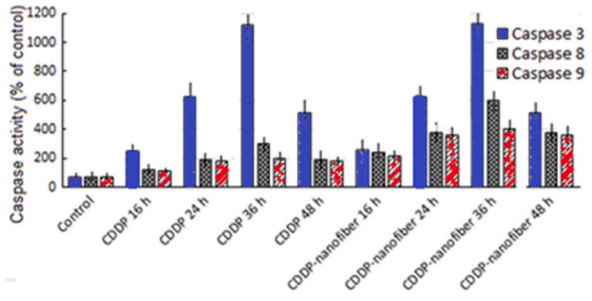

Fig. 11. Activation of caspases 3, 8 and 9 by CDDP and CDDP-nanofiber. The near confluent HepG2 cells were incubated for 16, 24, 36 or 48 h with 10 μM test sample and activity was recorded as % of the control. The values are the mean ± S.D. (n = 3).

only ~10 % at this time, indicating that the nanoformulation will deliver the drug to the colon. The release of cisplatin from the nanofibers followed the Higuchi kinetic model with $R^2 > 0.99$, which suggests diffusion- and solubility-controlled mechanism, whereas the release in contact with the cell line is due to hydrolysis of the drug. The cisplatin-loaded nanofibers exhibited significantly

($P < 0.05$) higher cytotoxic activity against the HepG2 cell line ($CC50 = 8 \pm 0.2\ \mu M$) than the standard cisplatin ($CC50 = 13 \pm 0.4\ \mu M$). In the caspase activity assay, caspase 3 was activated 16-fold by cisplatin compared to the control, whereas the activation of 8 and 9 was much lower (approximately 2-fold) than this. On the other hand, the cisplatin-loaded nanofibers activated caspase 3 to a slightly higher extent and 8 and 9 to double the extent (4-fold) of cisplatin, suggesting that the cisplatin-loaded nanofibers induce higher apoptotic activity than the standard cisplatin. The cisplatin-loaded nanofibers were thermally stabe up to 240 °C, meaning by that they can be steam sterilized. Thus, this nanoformulation can be considered a potential candidate for treatment of hepatocellular carcinoma as an implant.

Funding

This work was not supported by any funding agency.

Research involving human and animal rights

No animals were involved in this work.

Data and Code Availability

Please select why. Please note that this statement will be available alongside your article upon publication.
as follow-up to "**Data and Code Availability**.
Sharing research data helps other researchers evaluate your findings, build on your work and to increase trust in your article. We encourage all our authors to make as much of their data publicly available as reasonably possible. Please note that your response to the following questions regarding the public data availability and the reasons for potentially not making data available will be available alongside your article upon publication.
Has data associated with your study been deposited into a publicly available repository?
No data was used for the research described in the article.

CRediT authorship contribution statement

Anam Shabbir: Writing – original draft, Methodology, Investigation, Formal analysis, Data curation. **Mohammad Saeed Iqbal:** Writing – review & editing, Visualization, Validation, Supervision, Conceptualization. **Muhammad Zeeshan Saeed:** Writing – review & editing, Validation, Methodology. **Farooq Rashid:** Writing – review & editing, Validation, Methodology.

Declaration of competing interest

The authors declare that they have no known competing financial interests or personal relationships that could have appeared to influence the work reported in this paper.

Acknowledgement

Anam Shabbir was supported by a scholarship from Higher Education Commission of Pakistan under HEC Indigenous 5000 PhD Fellowship Program.

References

[1] A. Akhgari, Z. Heshmati, H. Afrasiabi Garekani, F. Sadeghi, A. Sabbagh, B. Sharif Makhmalzadeh, A. Nokhodchi, Indomethacin electrospun nanofibers for colonic drug delivery: in vitro dissolution studies, Colloids Surf. B Biointerfaces 152 (2017) 29–35, https://doi.org/10.1016/j.colsurfb.2016.12.035.
[2] M.H. El-Newehy, M.E. El-Naggar, S. Alotaiby, H. El-Hamshary, M. Moydeen, S. Al-Deyab, Preparation of biocompatible system based on electrospun CMC/PVA nanofibers as controlled release carrier of diclofenac sodium, J. Macromol. Sci., Pure Appl. Chem. 53 (2016) 566–573, https://doi.org/10.1080/10601325.2016.1201752.
[3] X. Hu, S. Liu, G. Zhou, Y. Huang, Z. Xie, X. Jing, Electrospinning of polymeric nanofibers for drug delivery applications, J. Contr. Release 185 (2014) 12–21, https://doi.org/10.1016/j.jconrel.2014.04.018.
[4] A. Morie, T. Garg, A.K. Goyal, G. Rath, Nanofibers as novel drug carrier - an overview, Artif. Cells, Nanomed. Biotechnol. 44 (2016) 135–143, https://doi.org/10.3109/21691401.2014.927879.
[5] A.A. El-Bindary, E.A. Toson, K.R. Shoueir, H.A. Aljohani, M.M. Abo-Ser, Metal–organic frameworks as efficient materials for drug delivery: synthesis, characterization, antioxidant, anticancer, antibacterial and molecular docking investigation, Appl. Organomet. Chem. 34 (2020), https://doi.org/10.1002/aoc.5905.
[6] M.A. El-Bindary, M.G. El-Desouky, A.A. El-Bindary, Metal–organic frameworks encapsulated with an anticancer compound as drug delivery system: synthesis, characterization, antioxidant, anticancer, antibacterial, and molecular docking investigation, Appl. Organomet. Chem. 36 (2022), https://doi.org/10.1002/aoc.6660.
[7] M.M. Abo-ser, E.-S.A. Toson, A.A. El-Bindary, G. Schlatter, K.R. Shoueir, Smart chitosan nanogel for targeted doxorubicin delivery, ensuring precise release, and minimizing side effects in Ehrlich ascites carcinoma-bearing mice, Int. J. Biol. Macromol. 267 (2024) 131390, https://doi.org/10.1016/j.ijbiomac.2024.131390.
[8] E. Entezar-Almahdi, R. Heidari, S. Ghasemi, S. Mohammadi-Samani, F. Farjadian, Integrin receptor mediated pH-responsive nano-hydrogel based on histidine-modified poly(aminoethyl methacrylamide) as targeted cisplatin delivery system, J. Drug Deliv. Sci. Technol. 62 (2021) 102402, https://doi.org/10.1016/j.jddst.2021.102402.

[9] S. Ghasemi, M. Owrang, F. Javaheri, F. Farjadian, Spermine modified PNIPAAm nano-hydrogel serving as thermo-responsive system for delivery of cisplatin, Macromol. Res. 30 (2022) 314–324, https://doi.org/10.1007/s13233-022-0035-7.

[10] K. Zarkesh, R. Heidari, P. Iranpour, N. Azarpira, F. Ahmadi, S. Mohammadi-Samani, F. Farjadian, Theranostic hyaluronan coated EDTA modified magnetic mesoporous silica nanoparticles for targeted delivery of cisplatin, J. Drug Deliv. Sci. Technol. 77 (2022) 103903, https://doi.org/10.1016/j.jddst.2022.103903.

[11] M. Abedi, S.S. Abolmaali, M. Abedanzadeh, F. Farjadian, S. Mohammadi Samani, A.M. Tamaddon, Core–shell imidazoline–functionalized mesoporous silica superparamagnetic hybrid nanoparticles as a potential theranostic agent for controlled delivery of platinum(II) compound, Int J Nanomedicine 15 (2020) 2617–2631, https://doi.org/10.2147/IJN.S245135.

[12] Y. Zhang, S. Liu, X. Wang, Z.Y. Zhang, X. Bin Jing, P. Zhang, Z.G. Xie, Prevention of local liver cancer recurrence after surgery using multilayered cisplatin-loaded polylactide electrospun nanofibers, Chin. J. Polym. Sci. 32 (2014) 1111–1118, https://doi.org/10.1007/s10118-014-1491-0.

[13] Y. Ma, X. Wang, S. Zong, Z. Zhang, Z. Xie, Y. Huang, Y. Yue, S. Liu, X. Jing, Local, combination chemotherapy in prevention of cervical cancer recurrence after surgery by using nanofibers co-loaded with cisplatin and curcumin, RSC Adv. 5 (2015) 106325–106332, https://doi.org/10.1039/c5ra17230f.

[14] J.A. Kaplan, R. Liu, J.D. Freedman, R. Padera, J. Schwartz, Y.L. Colson, M.W. Grinstaff, Prevention of lung cancer recurrence using cisplatin-loaded superhydrophobic nanofiber meshes, Biomaterials 76 (2016) 273–281, https://doi.org/10.1016/j.biomaterials.2015.10.060.

[15] Z. Nazemi, M. Sahraro, M. Janmohammadi, M.S. Nourbakhsh, H. Savoji, A review on tragacanth gum: a promising natural polysaccharide in drug delivery and cell therapy, Int. J. Biol. Macromol. 241 (2023) 124343, https://doi.org/10.1016/j.ijbiomac.2023.124343.

[16] S. Balaghi, M.A. Mohammadifar, A. Zargaraan, H.A. Gavlighi, M. Mohammadi, Compositional analysis and rheological characterization of gum tragacanth exudates from six species of Iranian Astragalus, Food Hydrocoll 25 (2011) 1775–1784, https://doi.org/10.1016/j.foodhyd.2011.04.003.

[17] M. Ghorbani, F. Mahmoodzadeh, L. Yavari Maroufi, P. Nezhad-Mokhtari, Electrospun tetracycline hydrochloride loaded zein/gum tragacanth/poly lactic acid nanofibers for biomedical application, Int. J. Biol. Macromol. 165 (2020) 1312–1322, https://doi.org/10.1016/j.ijbiomac.2020.09.225.

[18] M. Ghorbani, S. Ramezani, M.R. Rashidi, Fabrication of honey-loaded ethylcellulose/gum tragacanth nanofibers as an effective antibacterial wound dressing, Colloids Surf. A Physicochem. Eng. Asp. 621 (2021) 126615, https://doi.org/10.1016/j.colsurfa.2021.126615.

[19] M.R. Mohammadi, S. Rabbani, S.H. Bahrami, M.T. Joghataei, F. Moayer, Antibacterial performance and in vivo diabetic wound healing of curcumin loaded gum tragacanth/poly(ε-caprolactone) electrospun nanofibers, Mater. Sci. Eng. C 69 (2016) 1183–1191, https://doi.org/10.1016/j.msec.2016.08.032.

[20] C. Tang, M.J. Livingston, R. Safirstein, Z. Dong, Cisplatin nephrotoxicity: new insights and therapeutic implications, Nat. Rev. Nephrol. 19 (2023) 53–72, https://doi.org/10.1038/s41581-022-00631-7.

[21] L. Gao, S. Cai, A. Cai, Y. Zhao, T. Xu, Y. Ma, Y. Xu, Y. Wang, H. Wang, Y. Hu, The improved antitumor efficacy of continuous intratumoral chemotherapy with cisplatin-loaded implants for the treatment of sarcoma 180 tumor-bearing mice, Drug Deliv. 26 (2019) 208–215, https://doi.org/10.1080/10717544.2019.1574938.

[22] A. Shikanov, S. Shikanov, B. Vaisman, J. Golenser, A.J. Domb, Cisplatin tumor biodistribution and efficacy after intratumoral injection of a biodegradable extended release implant, Chemother Res Pract 2011 (2011) 1–9, https://doi.org/10.1155/2011/175054.

[23] L. Solorio, H. Wu, C. Hernandez, M. Gangolli, A.A. Exner, Ultrasound-guided intratumoral delivery of doxorubicin from *in situ* forming implants in a hepatocellular carcinoma model, Ther. Deliv. 7 (2016) 201–212, https://doi.org/10.4155/tde-2015-0008.

[24] A.K. Nayak, M.S. Hasnain, A.K. Dhara, S.C. Mandal, Herbal biopolysaccharides in drug delivery, in: Herbal Biomolecules in Healthcare Applications, Elsevier, 2022, pp. 613–642, https://doi.org/10.1016/B978-0-323-85852-6.00011-1.

[25] G.O. Aspinall, J. Baillie, Gum tragacanth. part i. fractionation of the gum and the structure of tragacanthic acid, J. Chem. Soc. (1963) 1696–1702, https://doi.org/10.1039/jr9630001702.

[26] Y. Bachra, A. Grouli, F. Damiri, M. Talbi, M. Berrada, A novel superabsorbent polymer from crosslinked carboxymethyl tragacanth gum with glutaraldehyde: synthesis, characterization, and swelling properties, Int J Biomater 2021 (2021) 1–14, https://doi.org/10.1155/2021/5008833.

[27] W.D. Holloway, C. Tasman-Jones, S.P. Lee, Digestion of certain fractions of dietary fiber in humans, Am. J. Clin. Nutr. 31 (1978) 927–930, https://doi.org/10.1093/ajcn/31.6.927.

[28] S. Moscato, F. Ronca, D. Campani, S. Danti, Poly(vinyl alcohol)/gelatin hydrogels cultured with HepG2 cells as a 3D model of hepatocellular carcinoma: a morphological study, J. Funct. Biomater. 6 (2015) 16–32, https://doi.org/10.3390/jfb6010016.

[29] M. Macka, J. Borák, L. Seménková, F. Kiss, Decomposition of cisplatin in aqueous solutions containing chlorides by ultrasonic energy and light, J Pharm Sci 83 (1994) 815–818, https://doi.org/10.1002/jps.2600830611.

[30] S.R.M.D. Morshed, T. Tokunaga, S. Otsuki, F. Takayama, T. Satoh, K. Hashimoto, T. Yasui, M. Okamura, J. Shimada, M. Kashimata, H. Sakagami, Effect of antitumor agents on cytotoxicity induction by sodium fluoride, Anticancer Res. 23 (2003) 4729–4736.

[31] M.M. Paradkar, J. Irudayaraj, A rapid FTIR spectroscopic method for estimation of caffeine in soft drinks and total methylxanthines in tea and coffee, J. Food Sci. 67 (2002) 2507–2511, https://doi.org/10.1111/j.1365-2621.2002.tb08767.x.

[32] E. Nazarzadeh Zare, P. Makvandi, F.R. Tay, Recent progress in the industrial and biomedical applications of tragacanth gum: a review, Carbohydr. Polym. 212 (2019) 450–467, https://doi.org/10.1016/j.carbpol.2019.02.076.

[33] P. Xu, E.A. Van Kirk, W.J. Murdoch, Y. Zhan, D.D. Isaak, M. Radosz, Y. Shen, Anticancer efficacies of cisplatin-releasing pH-responsive nanoparticles, Biomacromolecules 7 (2006) 829–835, https://doi.org/10.1021/bm050902y.

[34] U. Aggarwal, A.K. Goyal, G. Rath, Development and characterization of the cisplatin loaded nanofibers for the treatment of cervical cancer, Mater. Sci. Eng. C 75 (2017) 125–132, https://doi.org/10.1016/j.msec.2017.02.013.

[35] T. Higuchi, Mechanism of sustained-action medication. Theoretical analysis of rate of release of solid drugs dispersed in solid matrices, J Pharm Sci 52 (1963) 1145–1149, https://doi.org/10.1002/jps.2600521210.

[36] K. Nyberg, U. Johansson, I. Rundquist, P. Camner, Estimation of ph in individual alveolar macrophage phagolysosomes, Exp. Lung Res. 15 (1989) 499–510, https://doi.org/10.3109/01902148909069614.

[37] Z. Jing, R. Ni, J. Wang, X. Lin, D. Fan, Q. Wei, T. Zhang, Y. Zheng, H. Cai, Z. Liu, Practical strategy to construct anti-osteosarcoma bone substitutes by loading cisplatin into 3D-printed titanium alloy implants using a thermosensitive hydrogel, Bioact. Mater. 6 (2021) 4542–4557, https://doi.org/10.1016/j.bioactmat.2021.05.007.

[38] M. Okamura, K. Hashimoto, J. Shimada, H. Sakagami, Apoptosis-inducing activity of cisplatin (CDDP) against human hepatoma and oral squamous cell carcinoma cell lines, Anticancer Res. 24 (2004) 655–661.

[39] C.M.L. Mendoza, Y.T. Figueroa, M.G. Sánchez, M.M.C. Ortega, N.R. Fuentes, L.E.A. Quintana, In vitro evaluation and characterization of cisplatin loaded nanofibers for local chemotherapy, Discover Applied Sciences 6 (2024) 139, https://doi.org/10.1007/s42452-024-05631-9.

[40] G.-F. Zhuang, Y. Tan, Y.-Z. Yang, J.-W. Zhang, J. Tang, Experiment research of cisplatin implants inhibiting transplantation tumor growth and regulating the expression of KLK7 and E-cad of tumor-bearing mice with gastric cancer, Asian Pac J Trop Med 9 (2016) 606–609, https://doi.org/10.1016/j.apjtm.2016.04.022.

[41] M. Enari, R.V. Talanian, W.W. Wong, S. Nagata, Sequential activation of ICE-like and CPP32-like proteases during Fas-mediated apoptosis, Nature 380 (1996) 723–726, https://doi.org/10.1038/380723a0.

[42] P. Li, D. Nijhawan, I. Budihardjo, S.M. Srinivasula, M. Ahmad, E.S. Alnemri, X. Wang, Cytochrome c and dATP-dependent formation of Apaf-1/caspase-9 complex initiates an apoptotic protease cascade, Cell 91 (1997) 479–489, https://doi.org/10.1016/S0092-8674(00)80434-1.

[43] M. Müller, S. Strand, H. Hug, E.M. Heinemann, H. Walczak, W.J. Hofmann, W. Stremmel, P.H. Krammer, P.R. Galle, Drug-induced apoptosis in hepatoma cells is mediated by the CD95 (APO- 1/Fas) receptor/ligand system and involves activation of wild-type p53, J. Clin. Invest. 99 (1997) 403–413, https://doi.org/10.1172/JCI119174.

[44] S. Fulda, M. Los, C. Friesen, K.M. Debatin, Chemosensitivity of solid tumor cells in vitro is related to activation of the CD95 system, Int. J. Cancer 76 (1998) 105–114, https://doi.org/10.1002/(SICI)1097-0215(19980330)76:1<105::AID-IJC17>3.0.CO;2-B.
[45] Y. Mizutani, O. Yoshida, B. Bonavida, Sensitization of human bladder cancer cells to Fas-mediated cytotoxicity by cis-diamminedichloroplatinum (II), J. Urol. 160 (1998) 561–570, https://doi.org/10.1016/S0022-5347(01)62959-8.
[46] M.A. El-Bindary, A.A. El-Bindary, Synthesis, characterization, DNA binding, and biological action of dimedone arylhydrazone chelates, Appl. Organomet. Chem. 36 (2022), https://doi.org/10.1002/aoc.6576.